
Harnessing On-Device Large Language Model: Empirical Results and Implications for AI PC

Qingyu Song¹, Peiyu Liao², Wenqian Zhao², Yiwen Wang²
Shoubo Hu², Hui-Ling Zhen², Ning Jiang², Mingxuan Yuan²
¹The Chinese University of Hong Kong, ²Huawei

Abstract

The increasing deployment of Large Language Models (LLMs) on edge devices, driven by model advancements and hardware improvements, offers significant privacy benefits. However, these on-device LLMs inherently face performance limitations due to reduced model capacity and necessary compression techniques. To address this, we introduce a systematic methodology—encompassing model capability, development efficiency, and system resources—for evaluating on-device LLMs. Our comprehensive evaluation, encompassing models from 0.5B to 14B parameters and seven post-training quantization (PTQ) methods on commodity laptops, yields several critical insights: 1) System-level metrics exhibit near-linear scaling with effective bits-per-weight (BPW). 2) A practical threshold exists around ~ 3.5 effective BPW, larger models subjected to low-bit quantization consistently outperform smaller models utilizing higher bit-precision. 3) Quantization with low BPW incurs marginal accuracy loss but significant memory savings. 4) Determined by low-level implementation specifics power consumption on CPU, where computation-intensive operations spend more power than memory-intensive ones. These findings offer crucial insights and practical guidelines for the efficient deployment and optimized configuration of LLMs on resource-constrained edge devices. Our codebase is available at <https://github.com/simmonssong/LLMOnDevice>.

1 Introduction

Large language models (LLMs) have revolutionized modern applications through their advanced text-generation capabilities [1, 2]. While traditionally cloud-dependent, a paradigm shift towards on-device deployment is emerging [3, 4], enabled by breakthroughs in efficient model design [5] and advancements in edge computing hardware. This transition also addresses critical privacy concerns: on-device execution eliminates remote data transmission, positioning these models as essential tools for privacy-sensitive domains such as healthcare [6] and finance [7].

Despite these advantages, on-device LLMs face inherent limitations due to their reduced parameter count and the use of compression techniques like quantization and pruning [5], which restrict their performance potential [8]. Nonetheless, studies show they perform routine tasks—such as text summarization, intent recognition, and local query resolution—with adequate competence [9]. However, the lack of a comprehensive evaluation leaves their true capabilities underexplored. As these models evolve rapidly, establishing a comprehensive evaluation framework is crucial to ensure reliability, scalability, and alignment with user needs.

Numerous methods and readily available benchmarks have been proposed for evaluating the practical viability of LLMs for on-device deployment. For instance, MLPerf Client [10] evaluates Time to First Token (TTFT) and Tokens Per Second (TPS) for the 4-bit quantized Llama 2 model [11] across tasks inspired by real-world applications, such as content generation and text summarization. Similarly, LocalScore [12] assesses pre-filling throughput, text generation throughput, and TTFT for

4-bit quantized models of 1B, 8B, and 14B parameters. Power consumption metrics have also been explored, as demonstrated by Stevens et al. [13] who measure consumption in Watt-hours.

However, a common limitation is that most existing works typically concentrate on a subset of metrics, often evaluating accuracy, efficiency, or power consumption in isolation. While [14] concurrently evaluated output accuracy, inference performance, and energy efficiency, their analysis lacks a detailed examination of how these metrics are influenced by varying workloads (e.g., model size, token length) and specific methodologies (e.g., CPU operator implementations for quantization techniques).

To address these limitations, we propose a tripartite evaluation framework for on-device LLM inference that systematically considers: 1) *Model capability*: assessing task-specific accuracy using standardized benchmarks. 2) *Deployment efficiency*: quantifying generation throughput and latency under practical hardware constraints. 3) *System resource utilization*: analyzing resource consumption and potential contention, particularly in environments with concurrent applications. This multidimensional framework aims to provide a holistic understanding of the scenarios where, and methodologies by which, on-device LLMs can effectively serve as alternatives to cloud-based solutions.

Our investigation employs a representative consumer-grade Windows laptop with a single CPU and 16GB RAM, mirroring typical user hardware configurations. Through rigorous experimentation, we address three pivotal questions: 1) We establish the maximum model size that maintains acceptable system responsiveness during concurrent multitasking. 2) We dissect the trade-offs between quantization precision levels (4-bit to 8-bit) across our evaluation dimensions, revealing nonlinear relationships between bit-width reduction and performance degradation. 3) We compare different post-training quantization methods, demonstrating how algorithmic choices affect deployment outcomes. These findings provide actionable insights for optimizing the balance between model efficacy and resource efficiency in edge computing environments. Our primary contributions are:

Comprehensive Evaluation of On-Device LLM Inference: We conduct an extensive empirical study of LLM inference on edge devices using the Llama.cpp framework. The investigation encompasses eight LLMs of diverse parameter scales, subjected to seven distinct quantization methods. Model capability is benchmarked across five open-source datasets, while inference efficiency and resource utilization are assessed under four different input token lengths. This comprehensive methodology spans diverse model architectures, quantization levels, task types, and workloads.

Deployment Insights for Practical Scenarios: We offer actionable insights into the deployment of LLMs in production environments on edge devices. This includes an analysis of the trade-offs between task accuracy and deployment efficiency, guiding optimal model and quantization selection.

Guidance for LLM Inference Architecture and Acceleration: We provide recommendations for architectural optimizations pertinent to LLM inference frameworks. We offer insights for accelerating LLM inference on resource-constrained edge devices by analyzing potential bottlenecks, particularly the increasing communication overheads associated with larger model sizes.

2 Preliminaries

Quantization. Deploying LLMs on resource-constrained devices requires model compression [5], with post-training quantization being a leading strategy due to its ability to reduce model size and computational cost with minimal performance impact. A primary framework categorizes quantization methods into *symmetric* and *asymmetric* variants based on their alignment with the origin. Following [15], let $x \in \mathbb{R}$ be an original (pre-quantization) value and q its quantized counterpart, using $n \in \mathbb{N}^+$ bits of precision, symmetric quantization employs n -bit signed integers, where the discrete quantized value q lies in the range $\{-2^{n-1}, \dots, 2^{n-1} - 1\}$. A scaling factor $s \in \mathbb{R}$ is computed as $s = \frac{|x|_{\max}}{2^n - 1}$, where $|x|_{\max}$ is the maximum absolute value of x . Denoting rounding by $\text{Round}(\cdot)$, q is computed as

$$q = \max\left(-2^{n-1}, \min\left(\text{Round}\left(\frac{x}{s}\right), 2^{n-1} - 1\right)\right).$$

Asymmetric quantization employs n -bit unsigned integers, resulting in $q \in \{0, \dots, 2^n - 1\}$. Let $m = x_{\min}$ and x_{\max} be the minimum and maximum values of the input data x , respectively. The scaling factor s , which maps the input range $[m, x_{\max}]$ to approximately $[0, 2^n - 1]$, is computed as $s = \frac{x_{\max} - m}{2^n - 1}$. The input x is then quantized as $q = \max\left(0, \min\left(\text{Round}\left(\frac{x - m}{s}\right), 2^n - 1\right)\right)$.

Quantization methods in llama.cpp. llama.cpp [15] stands out as a crucial tool in the landscape of on-device LLM research and development due to its open-source and cross-platform nature.

The quantization schemes `n_0` and `n_k` implemented in `llama.cpp` is adopted in our study. The `n_0` method employs symmetric quantization, where weights are scaled uniformly using a zero-centered range, eliminating the need for zero-point offsets. In contrast, the `n_k` framework uses asymmetric strategy and further extends through five synergistic enhancements: 1) Hierarchical parameter grouping, which recursively quantizes scale s and offset m metadata to reduce overhead. 2) Activation-guided importance matrices that prioritize high-impact dimensions during quantization, mitigating accuracy loss from skewed weight distributions. 3) Post-quantization convex optimization to refine scales and zero-points by minimizing layer-wise reconstruction error. 4) Perturbative search algorithms that iteratively adjust quantized values to escape local minima, improving parameter recovery. 5) Heterogeneous bit allocation, assigning different precision to different weight matrices.

3 Methodology

This section outlines the evaluation methodology employed for on-device LLMs, encompassing the selection criteria for quantization methods and models, and the evaluation framework of 1) model capability, 2) deployment efficiency, and 3) system resource utilization, respectively.

3.1 Model and Quantization Selection

This study considers the Qwen 2.5 [16] and Llama 3 [17] series of LLMs due to their widespread adoption and popularity within the research community and industry. Specifically, Qwen 2.5 models with 0.5B, 1.5B, 3B, 7B, 14B parameters and Llama 3 models with 1.5B, 3B, 8B parameters are selected for evaluation. The upper limit of 14B parameters was chosen as it represents the largest model size that can be reliably deployed on a laptop equipped with 16GB of RAM after applying quantization techniques, enabling a practical on-device evaluation.

For effective on-device LLM deployment, both the quantization method and the resulting data format are critical considerations. The choice of quantization method, such as symmetric or asymmetric quantization, block-wise or per-tensor quantization, directly influences the trade-off between model size reduction and potential accuracy loss. The data format resulting from quantization, which dictates the bit-width and representation of the quantized weights, significantly impacts memory footprint and computational efficiency. Thus, considering the availability in `llama.cpp`, seven quantization methods i.e., `q8_0`, `q5_0`, `q4_0`, `q5_k`, `q4_k`, `q3_k`, and `q2_k`, are adopted in this study. Table 2 details a systematic comparison of these methods across key characteristics, where d_1 denotes primary layer, d_2 denotes secondary layer, and BPW denotes the resultant bits per weight.

3.2 Model Capability

Datasets. We have selected five diverse benchmarks that encompass a broad spectrum of competencies. GSM8K [18] emphasizes multi-step reasoning by presenting grade-school mathematics problems. HellaSwag [19] evaluates commonsense reasoning, challenging models to infer plausible continuations in everyday scenarios. Similarly, MMLU [20] spans a wide array of disciplines, providing an extensive evaluation of general knowledge. Together, these benchmarks facilitate a comprehensive assessment of a model’s performance, resilience, and adaptability under resource constraints. HumanEval [21] assesses the model’s capabilities in generating precise and efficient code, reflecting practical software development tasks. Lastly, TruthfulQA [22] examines the reliability of factual outputs and mitigates the risks related to hallucinated information.

Evaluation Metrics. Evaluation metrics for the aforementioned tasks must be tailored to their unique characteristics to ensure accurate and meaningful assessment of model performance. Each task presents distinct challenges and objectives, necessitating the use of specialized metrics that align with its specific requirements. Crafting task-specific evaluation metrics not only enhances the precision of benchmarking but also captures the nuanced capabilities of language models, ensuring holistic evaluation. Specific methodologies for metric construction per dataset are detailed in Appendix A.3.

We adopt `lm-evaluation-harness` [23] (version 0.4.8) as the evaluation tool to align with Open LLM Leaderboard so that all our evaluations and comparisons are fair and clear. Given the incomplete native support of `lm-evaluation-harness` (version 0.4.8) for `llama.cpp`, we develop a customized evaluation mechanism by extending `lm-evaluation-harness` to ensure comprehensive functionality. We keep the default settings on most hyper-parameters such as temperature and top- p

threshold. We set the same number of few shots according to the Qwen 2.5 technical report [16]: 4-shots for GSM8K [18], 10-shots for HellaSwag [19], 5-shots for MMLU [20], and 0-shot for TruthfulQA [22] and HumanEval [21]. To make the evaluation results consistent, the same fewshot setting is also applied to Llama 3 [17] models.

3.3 Deployment Efficiency

Datasets. To evaluate efficiency and sustained operational performance, we conduct text generation tasks employing extensive context sequences. These tasks utilize synthetic data generated by LLMs under evaluation. To simulate real-world application scenarios, initial inputs consist of text segments with lengths of 54, 118, 246, or 502 tokens. Each segment is prefixed with a constant 10-token instructional prompt (*Write a 50000-word article based on this text:*) to elicit long text generation. Thus, the total input lengths are 64, 128, 256, and 512 tokens, respectively. All generation processes are uniformly terminated upon reaching a maximum output length of 1024 tokens.

Evaluation Metrics. LLM inference efficiency is primarily evaluated by throughput (TPS), which is quantified independently for the pre-filling and decoding stages. Throughput is computed as the ratio between the number of tokens processed and the elapsed execution time. For the pre-filling stage, tokens correspond to input prompts, whereas for the decoding stage, tokens are those generated by the LLM. Execution time is directly obtained from the runtime logs provided by `llama.cpp`. To mitigate excessive latency associated with cold-start scenarios, we pre-warm the `llama.cpp` engine through three lightweight preliminary runs. Additionally, to ensure reproducibility and stable context generation, we fix both the `temperature` and `seed` parameters. In cases where token generation is insufficient, we adjust the values of `temperature` and `seed`, and subsequently repeat the experiment.

Throughput was determined by averaging results from three independent runs, each initiated after clearing the KV-cache to ensure reproducibility.

3.4 System Resource Utilization

Datasets. Consistent with the dataset configuration for efficiency evaluation (Section 3.3), 64, 128, 256, and 512 tokens are used as input to generate 1024 tokens.

Evaluation Metrics. Resource utilization is quantified by three primary metrics: CPU utilization, memory occupancy, and power consumption. Windows Performance Recorder (WPR) and Windows Performance Analyzer (WPA) are employed to systematically quantify and analyze system-level resource consumption throughout application execution, specifically monitoring CPU utilization, memory occupancy, and power draw. The `psutil` Python library is employed to quantify memory consumption. This library facilitates the retrieval of system and process information, including detailed memory usage statistics. Our analysis focuses on the Resident Set Size (RSS), representing the non-swapped physical memory utilized by the LLM inference process. The key metric adopted is Peak RSS, defined as the maximum physical RAM consumed by the process at any point during its execution, thereby capturing the worst-case memory footprint. The specific `psutil` metric for RSS on Windows corresponds to the “`wset`” field, aligning with the “Memory (Working Set)” in Task Manager, consistent with system-level reporting.

Energy consumption is assessed using the Windows Energy Estimation Engine (E3), an integrated real-time power modeling system. E3 translates hardware activity metrics into energy estimates for various system components. To optimize data collection and minimize extraneous recording, a customized Windows Performance Recorder (WPR) profile is developed through a structured XML configuration. This tailored profile enables targeted logging of energy-relevant counters.

4 Experiments

Experiments are conducted using `llama-cpp-python` [24] (version 0.3.7), an open-source Python binding for `llama.cpp`. The evaluation platform comprises a consumer-grade laptop featuring a 13th-generation Intel® Core™ i7-1360P CPU (12 cores, 2.20 GHz base frequency) and 16 GB RAM, chosen to emulate typical user hardware configurations.

Based on the assumption that the model exhibits only minimal task performance differences between CPU and GPU platforms [25], and considering the significantly inferior inference throughput of

Table 1: Performance of selected Qwen 2.5 [16] instruction-tuned models.

Models & Tasks		fp16	q8_0	q5_k	Quantization				
					q5_0	q4_k	q4_0	q3_k	q2_k
14B	GSM8K [18]	/	/	89.08	89.76	88.86	90.45	89.01	84.46
	HellaSwag [19]	/	/	85.09	84.78	84.72	84.24	83.93	81.76
	MMLU [20]	/	/	79.74	79.75	79.55	79.43	78.86	75.74
	HumanEval [21]	/	/	69.51	69.51	68.90	68.90	69.51	62.20
	TruthfulQA [22]	/	/	68.64	69.63	68.93	67.50	66.92	65.89
7B	GSM8K [18]	/	86.73	86.05	87.11	85.52	86.20	84.46	76.19
	HellaSwag [19]	/	81.32	81.21	81.19	80.94	80.59	79.79	77.48
	MMLU [20]	/	74.24	74.27	74.15	74.26	74.04	73.23	68.58
	HumanEval [21]	/	70.73	67.68	68.90	64.63	58.54	63.41	53.66
	TruthfulQA [22]	/	64.74	64.25	64.45	63.80	62.22	64.44	62.25
3B	GSM8K [18]	80.89	80.29	78.77	80.82	76.80	75.36	62.62	48.52
	HellaSwag [19]	75.29	75.07	74.90	75.10	74.86	73.69	70.85	68.56
	MMLU [20]	66.38	66.52	66.06	66.34	65.68	65.08	60.15	58.80
	HumanEval [21]	54.88	54.88	49.39	47.56	48.78	45.12	46.34	31.10
	TruthfulQA [22]	58.67	58.59	58.38	58.94	58.38	57.00	56.38	50.16
1.5B	GSM8K [18]	60.80	59.82	59.14	57.85	52.77	53.30	46.47	21.46
	HellaSwag [19]	67.91	67.92	67.70	67.66	66.81	66.89	65.06	59.92
	MMLU [20]	60.28	60.36	60.32	59.77	59.76	59.14	57.33	51.30
	HumanEval [21]	37.20	37.80	34.76	39.02	37.50	35.37	24.39	20.73
	TruthfulQA [22]	46.70	46.70	45.78	46.41	45.41	47.71	45.21	46.51
0.5B	GSM8K [18]	31.48	33.28	31.77	30.86	30.33	21.00	25.85	21.99
	HellaSwag [19]	50.50	50.37	49.88	50.12	50.20	48.52	49.65	49.04
	MMLU [20]	46.69	46.81	46.09	46.08	46.12	44.36	45.53	44.83
	HumanEval [21]	29.88	31.71	26.83	29.27	28.66	22.56	28.05	25.00
	TruthfulQA [22]	42.50	42.50	42.15	42.61	42.51	40.40	41.89	40.90

LLMs deployed on CPUs, we have strategically assigned all task performance evaluation tasks to the GPU device due to computational efficiency. For task performance evaluation, the experiments were performed on a Linux workstation featuring two Intel® Xeon® Platinum 8480C CPUs (each 56 cores, max 3.80 GHz) and a single NVIDIA H800 GPU with 80 GB of VRAM.

4.1 Model Capability Results

Following the experimental setup in Section 3.3, we showcase the performance of selected Qwen2.5 [16] instruction-tuned models, ranging in sizes from 1.5B to 14B parameters, across aforementioned tasks GSM8K [18], HellaSwag [19], MMLU [20], HumanEval [21], and TruthfulQA [22] in Table 1. For each model, we evaluate the original fp16 model (except 7B and 14B) with a series of quantization levels following the experimental setup introduced in Section 3.2. The results highlight the impact of both model size and quantization methods on task accuracy. From Table 1, a clear trend emerges showing that larger models in parameters generally achieve higher accuracy across almost all tasks, demonstrating their greater capacity for reasoning, knowledge retention, and adaptability. For example, the 14B models consistently outperform the smaller models, with different quantization series yielding top scores on GSM8K [18] (q4_0), HellaSwag [19] (q5_k), MMLU [20] (q5_0), and TruthfulQA [22] (q5_0). Smaller models, such as the 3B and 1.5B variants, show a noticeable decline in accuracy, particularly on reasoning-intensive tasks like GSM8K and MMLU. It is notable that the 7B models, particularly the q8_0 model, achieve results on HumanEval [21] that are comparable to, and even slightly better than, some of the 14B models. While this might seem counterintuitive at first, such behavior is also observed in [16].

Within each model size, the choice of quantization has a substantial impact on performance. The fp16 model generally achieves the highest accuracy, suggesting that lower quantization levels may degrade performance due to precision loss. Additionally, the results reveal that larger models are more robust to variations in quantization levels compared to smaller models. For example, the 14B model on GSM8K [18] demonstrates only a slight reduction in accuracy, from 89.08% (q5_k) to 89.01% (q3_k). In contrast, the 1.5B model shows a more pronounced decline, with its accuracy decreasing from 59.14% (q5_k) to 46.47% (q3_k). The findings from Table 1 indicate that larger models are more resilient to performance loss caused by lower-precision quantization. However, the q2_k configuration significantly degrades performance across all model sizes, demonstrating

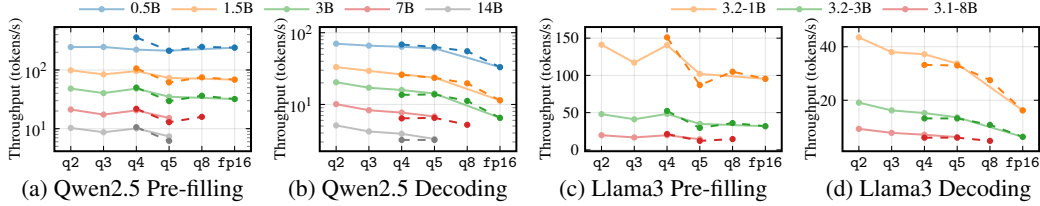


Figure 1: Pre-filling and decoding throughput of selected models of Qwen 2.5 [16] and Llama 3 [17] against different quantization methods (128-token input).

that extreme quantization harms both computational accuracy and representation fidelity. These results highlight the robustness of larger models, likely due to their higher parameter capacity, and offer insights for optimizing quantization in smaller models to ensure usability in resource-limited environments, such as on-device LLMs.

Moreover, task-specific performance provides insights into the models’ strengths and weaknesses. Tasks like HumanEval [21], which involve code generation, exhibit greater sensitivity to model size and quantization. For example, the accuracy for HumanEval drops sharply in smaller models, with the 1.5B q5_0 model achieving 39.02% compared to 69.51% in the 14B counterpart. TruthfulQA [22] similarly shows a decline in factual reliability as model size decreases, highlighting the challenges of maintaining accuracy in smaller models.

4.2 Deployment Efficiency Results

We showcase the pre-filling and decoding efficiencies of selected instruction-tuned models of Qwen 2.5 [16] and Llama 3 [17] across the quantization series introduced in Section 3.1. We highlight the impact of model size, prompt length, and quantization methods on efficiency.

Figure 1 depicts throughput as a function of model size with 128 input tokens. Solid bold curves correspond to the n_k quantization family, while dashed curves indicate the n_0 family. Individual models, detailed in Section 3.1, are distinguished by color. Two primary trends are evident: 1) A monotonic decline in throughput is observed with increasing model scale. 2) The choice of quantization method exerts a diminishing influence at larger model scales. These findings suggest that when deploying LLMs on resource-constrained devices, higher BPW quantization methods offer a balance between accuracy and computational cost, preserving accuracy with a minimal latency penalty.

Impact of Quantization Method. Moreover, we analyze the impact of quantization technique on throughput. During decoding (Figures 5b and 5d), throughput declines monotonically with increasing BPW, as higher-precision quantization methods entail greater computational and memory traffic overhead. This effect is considerably more pronounced than during the pre-filling phase (Figures 5a and 5c), consistent with decoding being predominantly memory-bound. Further, operator-level optimizations within `llama.cpp` amplify the performance advantage of the n_k series; for both 4-bit and 5-bit configurations, n_k variants outperform their n_0 counterparts.

During the pre-filling phase (Figures 5a and 5c), throughput consistently decreases as BPW increases. However, since pre-filling is compute-bound, the impact of CPU computational overhead is magnified relative to the decoding phase. Specifically, the q5_k quantization scheme achieves a greater speedup relative to q5_0 due to its integration of 6-bit quantization within its 5-bit framework. Both methods partition quantized weights across multiple bytes. The 6-bit quantization component within q5_k requires fewer data concatenation iterations to form 8-bit or 16-bit data units during the unpacking process [26]. Conversely, this mixed-precision approach, characteristic of n_k variants, introduces additional bit-shifting operations. For instance, while the q4_0 method employs a single shifting operation to unpack quantized weights into an 8-bit data unit, the more complex unpacking logic in q4_k (and other _k schemes) may result in slightly reduced throughput compared to the simpler q4_0. q2_k and q3_k necessitate even more shifting operations and iterations, leading to lower throughput compared to 4-bit methods (q4_k and q4_0). However, for very small models, such as Qwen 2.5 0.5B (Figure 5a), low-bit quantization can improve cache hit rates, thereby enhancing throughput. Thus, in such cases, the increased computational overhead associated with complex unpacking can be offset by gains in memory access efficiency.

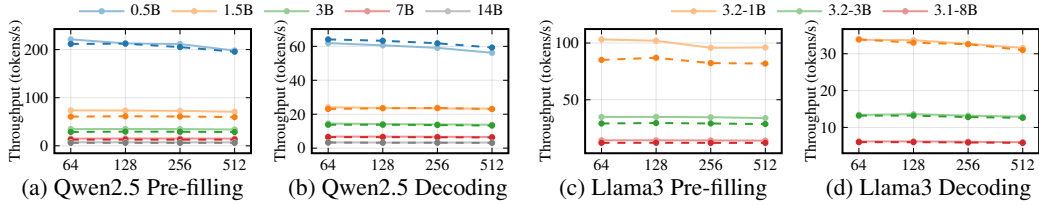


Figure 2: Pre-filling and decoding throughput with selected models of Qwen 2.5 [16] and Llama 3 [17] against different token lengths (5-bit quantization).

Impact of Token Length. Figure 2 illustrates throughput performance as a function of model size under 5-bit quantization schemes (q5_k and q5_0). During decoding, a fixed output length of 1024 tokens is employed. The observed marginal decrease (3% on 14B and 7B, 5% on 3B) in throughput with increasing token length indicates minimal growth in communication or computation overheads, suggesting neither currently constitutes the primary bottleneck. Regarding communication, model weight transmission overhead is dominant for shorter token sequences, as the incremental communication cost of the KV-cache is negligible relative to that of the model weights. Conversely, for smaller models, an increasing proportion of KV-cache communication, relative to model weight transmission, results in a more significant throughput degradation (7% on 1B, 9% on 0.5B).

Figures 1 and 2 reveals distinct throughput degradation patterns between small and large models. For small models, Figure 1 indicates that quantization schemes with higher BPW exhibit less severe throughput degradation. This suggests a greater dominance of communication over computation within these smaller model architectures. This communication dominance is further corroborated by Figure 2, where, for small models, throughput degradation is also mitigated with increasing input token lengths. Consequently, the primary performance bottleneck—whether computation or communication—is contingent upon model size, particularly when considering the computational limitations of CPUs and the communication constraints inherent to edge devices.

4.3 System Resource Utilization Results

To investigate the computational efficiency of quantized LLMs on edge devices, we first analyze the CPU power consumption across varying bit-widths and model scales. As shown in Figure 3a, the overall CPU power remains relatively stable across quantization levels (q2_k to q8_0), fluctuating within a narrow range of 7.9 to 9.5W. Notably, on average q4_0 and q8_0 exhibit marginally higher power consumption (9.2W and 9.5W) compared to q5_0 (8.5W), suggesting subtle efficiency differences in processing mixed-precision operations. This phenomenon may stem from hardware-level optimizations for specific bit-width arithmetic units—for instance, q5_0’s alignment with 32-bit register boundaries could reduce instruction pipeline stalls, whereas q4_0’s irregular bit grouping might introduce additional cycle overhead for bit-unpacking operations.

A more pronounced trend emerges when visualizing the interaction between model size and quantization bit-width in Figure 3a. Quantization bit-width significantly modulates the relationship between model scale and CPU power consumption. At q2_k precision, larger models paradoxically demonstrate lower power usage: the 7B model consumes 8.27W versus 9.33W for 0.5B (↑1.06W). This trend disappears at q8_0, where the 7B and 0.5B models exhibit minimal divergence (9.31W vs. 9.65W, ↑0.34W). We observe two key patterns: 1) Ultra-low bit quantization (q2_k) enables memory access optimization for larger models (e.g., reduced cache misses due to full weight residency), overriding computational load increases; 2) High-bit operations (q8_0) saturate CPU arithmetic units regardless of model scale, diminishing size-related efficiency variations. The results suggest that aggressive quantization shifts power bottlenecks from computation to memory subsystems, with diminishing returns as bit-width increases. Memory consumption scales near-monotonically with quantization bit-width across model sizes except for q4_0. For example, 0.5B models grow from 392 MB (q2_k) to 576 MB (q8_0), while 7B models expand from 2411 MB to 7297 MB. The q4_0 scheme deviates from this trend, exhibiting higher memory usage than adjacent bit-widths (e.g., 0.5B q4_0 at 597 MB vs. q5_0 at 448 MB). This anomaly persists across scales, with 7B q4_0 requiring 6910 MB versus an expected value between 3535 MB (q3_k) and 4837 MB (q5_0). We trace this anomaly to runtime weight repacking—an optimization that reorganizes 4-bit groups into computation-friendly 32-bit aligned blocks. This design choice prioritizes computational efficiency over minimal memory use and

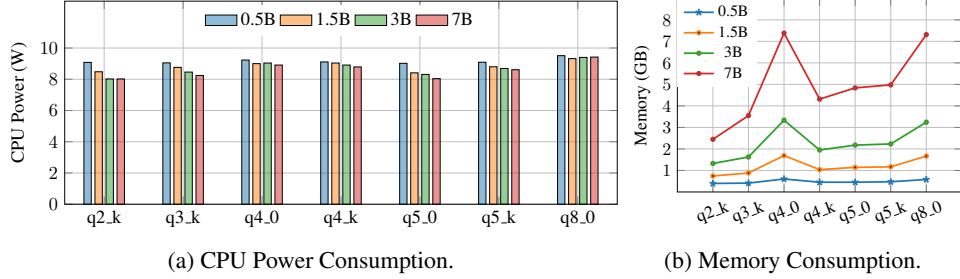


Figure 3: System resource utilization (power in Watt and memory in GB) of Qwen 2.5 series (from 0.5B to 7B). Prompt size of 128 tokens and output size 1000 tokens are fixed.

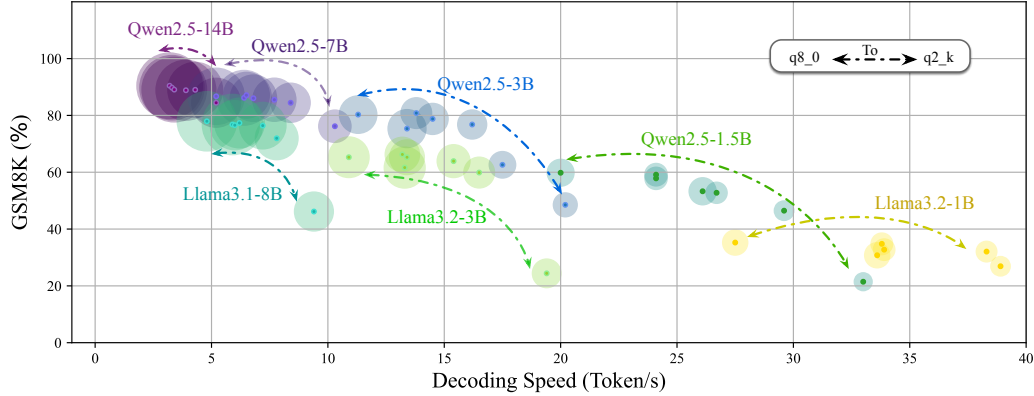


Figure 4: Visualisation of decoding speed (token/s) and model performance (GSM8K score). Llama 3 and Qwen 2.5 series are evaluated at different quantization scheme (q8_0 to q2_k). The circle area of each model is proportional to its memory consumption on device.

is adopted specifically for q4_0 in Llama.cpp. The otherwise consistent linear progression confirms that non-exceptional quantization methods maintain predictable memory scaling proportional to bit-width.

As depicted in Figure 3, q4_0 exhibits higher power consumption than q4_k, whereas q5_0 demonstrates lower power consumption relative to q5_k. The elevated power consumption of q4_0 compared to q4_k is attributed to increased CPU utilization during prefilling, whose simpler de-quantization method enhances computational efficiency in compute-bound scenarios. Conversely, the reduced power consumption of q5_0 relative to q5_k stems from lower CPU utilization during decoding, a consequence of its more memory-intensive workload, as detailed in Figure 13. Further, q4_k, q4_0, and q8_0 manifest significantly higher power consumption than other quantized models, primarily due to greater CPU utilization during the decoding phase (Figure 13). Conversely, low-bit quantized models (q2_k, q3_k, q5_0) exhibit reduced power consumption, driven by three key factors: higher SA power (reflecting memory-intensive workloads), lower CPU frequencies (reducing dynamic power), and diminished CPU utilization during decoding due to increased memory access intensity (Figure 13). Power consumption on CPU is primarily determined by low-level implementation details rather than high-level model characteristics such as quantization, model size, or architecture. This is because computation-intensive operations typically consume significantly more power than memory-intensive ones. Further, the interplay among these three metrics (accuracy, speed, and memory consumption) is evaluated. As illustrated in Figure 4 plotting GSM8K accuracy (y-axis) versus decoding speed (x-axis) with bubble sizes encoding memory consumption, we identify three key trends: First, Qwen 2.5 models consistently dominate the Pareto frontier, outperforming Llama variants in both accuracy and speed across all tested scales. Quantitative analysis reveals that compressing models to 4-bit precision preserves near-baseline accuracy while accelerating inference by 30-50%, with memory reductions remaining secondary to speed improvements. Below 4-bit, however, severe accuracy degradation occurs despite additional speed gains. Second, scale-dependent robustness is evident: Qwen 2.5 7B maintains comparable accuracy to its 14B counterpart with doubled inference speed, while sub-3B models exhibit disproportionately larger accuracy losses even with computational advantages. Critically, model scale fundamentally governs the trade-off landscape

more than quantization strategies. Scaling from 7B to 14B parameters significantly sacrifices speed for accuracy gains, whereas equivalent memory reductions via 4-bit quantization achieve speed improvements with negligible accuracy loss. This underscores model architecture scaling as the primary determinant of deployment efficiency-accuracy equilibria, with quantization acting as a supplemental tool for memory/speed refinement.

5 Conclusion and Discussion

This paper presents a systematic evaluation of LLM inference on edge devices. Our experimental results yield several key findings concerning model capability, deployment efficiency, and system resource utilization across diverse model sizes and quantization methods.

Model Capability. Model capability increases monotonically with BPW and model scale. Qwen models generally outperform Llama models. Further, large models employing low-bit quantization demonstrate superior performance compared to smaller models utilizing higher-bit quantization.

Deployment Efficiency. A primary observation is that throughput consistently decreases with increasing model size. Moreover, the impact of BPW on throughput differs between the pre-filling and decoding phases. During decoding, data communication bottlenecks typically lead to a monotonic decrease in throughput with increasing BPW. However, the computational demands imposed by different quantization methods also significantly influence throughput. For a given bit-width, while de-quantization and forward computation are largely consistent, the efficiency of the unpacking operation emerges as a critical determinant of throughput. Quantization methods involving fewer discrete operations (e.g., bit-shifting, logical iterations) generally yield higher throughput. However, for sufficiently small models, improved cache hit rates and reduced model/KV-cache footprints can alleviate communication bottlenecks, potentially enhancing throughput as model size diminishes.

During the pre-filling phase, the dense computations inherent to batch processing typically render the system computation-bound, particularly for large models. Consequently, the computational efficiency of the selected quantization method becomes paramount for throughput in these scenarios. Conversely, for small models during pre-filling, which are generally less computation-bound, effective management of communication overheads—facilitated by smaller model and KV-cache sizes—is crucial for optimizing throughput.

System Resource Utilization. Memory consumption exhibits a monotonic increase with BPW. Quantization methods characterized by fewer CPU operations during the unpacking stage generally correlate with higher overall CPU utilization, as computational throughput is less frequently impeded by this process compared to less efficient alternatives.

The observations lead to the following insights, offered as recommendations for model and quantization method selection, particularly for on-device framework development and efficiency optimization:

Trade-off between Model Capability and Deployment Efficiency. For large-scale models, low-bit-width quantization typically preserves accuracy while offering only marginal gains in deployment efficiency. Conversely, for small-scale models, low-bit-width quantization can maintain comparable accuracy while substantially improving deployment efficiency.

Model Selection for Resource-Constrained Scenarios: In scenarios prioritizing accuracy, the deployment of *large models with moderate quantization precision* (e.g., 4-bit) is often advisable, as this frequently represents an optimal balance among capability, efficiency, and resource consumption. Conversely, in scenarios where deployment efficiency is paramount, employing *small models, also with moderate quantization precision*, can be more effective.

Bottleneck Identification on Edge Devices: CPUs on edge devices are susceptible to becoming computation-bound, particularly with larger models. Even during decoding, limitations in concurrent processing capabilities can render computation the dominant factor limiting throughput for models exceeding approximately 1B parameters. Consequently, optimizing computational efficiency is crucial for these larger models. In contrast, for models smaller than approximately 0.5B parameters, communication overhead typically governs inference efficiency; therefore, enhancements in data transfer efficiency will yield more substantial throughput gains in such cases.

References

- [1] Josh Achiam, Steven Adler, Sandhini Agarwal, Lama Ahmad, Ilge Akkaya, Florencia Leoni Aleman, Diogo Almeida, Janko Altenschmidt, Sam Altman, Shyamal Anadkat, et al. Gpt-4 technical report. *arXiv preprint arXiv:2303.08774*, 2023.
- [2] Aixin Liu, Bei Feng, Bing Xue, Bingxuan Wang, Bochao Wu, Chengda Lu, Chenggang Zhao, Chengqi Deng, Chenyu Zhang, Chong Ruan, et al. Deepseek-v3 technical report. *arXiv preprint arXiv:2412.19437*, 2024.
- [3] Wei Chen and Zhiyuan Li. Octopus v3: Technical report for on-device sub-billion multimodal ai agent. *arXiv preprint arXiv:2404.11459*, 2024.
- [4] Shengding Hu, Yuge Tu, Xu Han, Chaoqun He, Ganqu Cui, Xiang Long, Zhi Zheng, Yewei Fang, Yuxiang Huang, Weilin Zhao, et al. MiniCPM: Unveiling the potential of small language models with scalable training strategies. *arXiv preprint arXiv:2404.06395*, 2024.
- [5] Xunyu Zhu, Jian Li, Yong Liu, Can Ma, and Weiping Wang. A survey on model compression for large language models. *Transactions of the Association for Computational Linguistics*, 12:1556–1577, 11 2024.
- [6] Arun James Thirunavukarasu, Darren Shu Jeng Ting, Kabilan Elangovan, Laura Gutierrez, Ting Fang Tan, and Daniel Shu Wei Ting. Large language models in medicine. *Nature medicine*, 29(8):1930–1940, 2023.
- [7] Shijie Wu, Ozan Irsoy, Steven Lu, Vadim Dabravolski, Mark Dredze, Sebastian Gehrmann, Prabhajan Kambadur, David Rosenberg, and Gideon Mann. Bloomberggpt: A large language model for finance. *arXiv preprint arXiv:2303.17564*, 2023.
- [8] Jiajun Xu, Zhiyuan Li, Wei Chen, Qun Wang, Xin Gao, Qi Cai, and Ziyuan Ling. On-device language models: A comprehensive review. *arXiv preprint arXiv:2409.00088*, 2024.
- [9] Gemma Team, Aishwarya Kamath, Johan Ferret, Shreya Pathak, Nino Vieillard, Ramona Merhej, Sarah Perrin, Tatiana Matejovicova, Alexandre Ramé, Morgane Rivière, et al. Gemma 3 technical report. *arXiv preprint arXiv:2503.19786*, 2025.
- [10] MLCommons Association. MLPerf® Client Benchmark: Version 0.6. <https://mlcommons.org/2025/04/mlperf-client-v0-6/>, April 2025.
- [11] Hugo Touvron, Louis Martin, Kevin Stone, Peter Albert, Amjad Almahairi, Yasmine Babaei, Nikolay Bashlykov, Soumya Batra, Prajjwal Bhargava, Shruti Bhosale, et al. Llama 2: Open foundation and fine-tuned chat models. *arXiv preprint arXiv:2307.09288*, 2023.
- [12] C. J. Pais. Introducing LocalScore: A local LLM benchmark. <https://www.localscore.ai/blog>, April 2025. Blog post, Mozilla Builders project.
- [13] Didier Stevens. Quickpost: The Electric Energy Consumption of LLMs. <https://blog.didierstevens.com/2024/10/06/quickpost-the-electric-energy-consumption-of-llms/>, October 2024. Blog post.
- [14] Erik Johannes Husom, Arda Goknil, Merve Astekin, Lwin Khin Shar, Andre Kåsen, Sagar Sen, Benedikt Andreas Mithassel, and Ahmet Soyly. Sustainable llm inference for edge ai: Evaluating quantized llms for energy efficiency, output accuracy, and inference latency. *arXiv preprint arXiv:2504.03360*, 2025.
- [15] ggml-org. ggml: Tensor library for machine learning. <https://github.com/ggml-org/llama.cpp>, 2024. Commit 5555c0c.
- [16] Qwen Team. Qwen2.5 technical report. *arXiv preprint arXiv:2412.15115*, 2024.
- [17] Llama Team. The Llama 3 herd of models. *arXiv preprint 2407.21783*, 2024.
- [18] Karl Cobbe, Vineet Kosaraju, Mohammad Bavarian, Mark Chen, Heewoo Jun, Łukasz Kaiser, Matthias Plappert, Jerry Tworek, Jacob Hilton, Reiichiro Nakano, et al. Training verifiers to solve math word problems. *arXiv preprint arXiv:2110.14168*, 2021.

- [19] Rowan Zellers, Ari Holtzman, Yonatan Bisk, Ali Farhadi, and Yejin Choi. HellaSwag: Can a machine really finish your sentence? In *Proceedings of the 57th Annual Meeting of the Association for Computational Linguistics*, pages 4791–4800, 2019.
- [20] Dan Hendrycks, Collin Burns, Steven Basart, Andy Zou, Mantas Mazeika, Dawn Song, and Jacob Steinhardt. Measuring massive multitask language understanding. In *International Conference on Learning Representations*, 2021.
- [21] Mark Chen, Jerry Tworek, Heewoo Jun, Qiming Yuan, Henrique Ponde De Oliveira Pinto, Jared Kaplan, Harri Edwards, Yuri Burda, Nicholas Joseph, Greg Brockman, et al. Evaluating large language models trained on code. *arXiv preprint arXiv:2107.03374*, 2021.
- [22] Stephanie Lin, Jacob Hilton, and Owain Evans. TruthfulQA: Measuring how models mimic human falsehoods. In *Proceedings of the 60th Annual Meeting of the Association for Computational Linguistics (Volume 1: Long Papers)*, pages 3214–3252, 2022.
- [23] Leo Gao, Jonathan Tow, Baber Abbasi, Stella Biderman, Sid Black, Anthony DiPofi, Charles Foster, Laurence Golding, Jeffrey Hsu, Alain Le Noac’h, Haonan Li, Kyle McDonell, Niklas Muennighoff, Chris Ociepa, Jason Phang, Laria Reynolds, Hailey Schoelkopf, Aviya Skowron, Lintang Sutawika, Eric Tang, Anish Thite, Ben Wang, Kevin Wang, and Andy Zou. A framework for few-shot language model evaluation, 07 2024.
- [24] Andrei. llama-cpp-python. <https://github.com/abetlen/llama-cpp-python>, 2024. Version 0.3.7.
- [25] Alex Schlögl, Nora Hofer, and Rainer Böhme. Causes and effects of unanticipated numerical deviations in neural network inference frameworks. *Advances in Neural Information Processing Systems*, 36:56095–56107, 2023.
- [26] marcingomulkiewicz. (stupid?) q6/5 quantization idea. github.com/ggerganov/llama.cpp/discussions/9539, 2024.
- [27] DavidZyy. Introduction of quantization methods in llama.cpp. <https://zhuanlan.zhihu.com/p/12729759086>, 2024.
- [28] jukofyork. Empirical correction of imatrix in llama.cpp. <https://github.com/ggml-org/llama.cpp/discussions/5263#discussioncomment-11511794>, 2024.
- [29] ggml-org. ggml: Tensor library for machine learning. <https://github.com/ggml-org/ggml>, 2023. Commit ff90433.

A Appendix

A.1 Details of Importance Matrix

To reduce the precision degradation between de-quantized and pre-quantized values, `llama.cpp` [15] formulates an optimization problem that leverages activation statistics to construct weight-aware objective functions. Let $\mathbf{w} \in \mathbb{R}^d$ denote a d -dimensional learnable parameter vector, with $\mathbf{q} \in \mathbb{Q}^d$ representing its quantized counterpart obtained through standard quantization procedures. Let $\mathbf{a} \in \mathbb{R}^d$ denotes the corresponding activation vector from the preceding layer. For each dimension $i \in \{1, 2, \dots, d\}$, the per-block quantization problem can be formulated as a quadratic programming problem as $\min_{s,m} \mathbb{E} \left[\sum_{i=1}^d (\mathbf{q}_i - \mathbf{w}_i) \mathbf{a}_i \right]^2$ (s and m are the scale factor and the minimum value defined in Section 2). Taking the reformulation in [27], the sum-squared operation in the objective above can be simplified into squared-sum form as:

$$\mathbb{E} \left[\sum_{i=1}^d (\mathbf{q}_i - \mathbf{w}_i) \mathbf{a}_i \right]^2 \approx \mathbb{E} \left[\sum_{i=1}^d \mathbf{a}_i^2 (\mathbf{q}_i - \mathbf{w}_i)^2 \right], \quad (1)$$

where the coefficient \mathbf{a}_i serves as a weighting factor in the optimization objective.

Proof.

$$\begin{aligned} & \mathbb{E} \left[\sum_{i=1}^d (\mathbf{q}_i - \mathbf{w}_i) \mathbf{a}_i \right]^2 \\ \text{Expansion of quadratic} & \implies = \mathbb{E} \left[\sum_{i=1}^d ((\mathbf{q}_i - \mathbf{w}_i) \mathbf{a}_i)^2 + \sum_{j=1, j \neq i}^d (\mathbf{q}_i - \mathbf{w}_i) \mathbf{a}_i (\mathbf{q}_j - \mathbf{w}_j) \mathbf{a}_j \right], \\ \text{Sum of expectation} & \implies = \mathbb{E} \left[\sum_{i=1}^d ((\mathbf{q}_i - \mathbf{w}_i) \mathbf{a}_i)^2 \right] + \mathbb{E} \left[\sum_{j=1, j \neq i}^d (\mathbf{q}_i - \mathbf{w}_i) \mathbf{a}_i (\mathbf{q}_j - \mathbf{w}_j) \mathbf{a}_j \right], \\ \text{Eliminate Second Term} & \implies \approx \mathbb{E} \left[\sum_{i=1}^d \mathbf{a}_i^2 (\mathbf{q}_i - \mathbf{w}_i)^2 \right]. \end{aligned}$$

□

Empirical studies suggest that parameters with larger magnitudes exhibit greater influence in neural network computations [28]. To amplify the significance of these salient parameters, a squared magnitude term x_i^2 is incorporated into the weighting factor [28]. x_i^2 also serves as a simple approximation of the diagonal entries of Hessian matrices [28]. Moreover, to address numerical instability in low-magnitude regimes, block-wise mean squared value of original data is calculated as $\sigma_2 = \frac{1}{n} \sum_{i=1}^n \mathbf{x}_i^2$ [28]. This regularization prevents the systematic underestimation of near-zero parameters during quantization [28]. The complete importance matrix is therefore formulated as $\tilde{\mathbf{a}}_i^2 = \mathbf{a}_i^2 \sqrt{\sigma_2 + \mathbf{x}_i^2}$.

A.2 Details of Selected Quantization Methods of `llama.cpp` [29]

We begin by introducing the *mini-block technique* utilized in `llama.cpp`, which enhances data representation fidelity by quantizing parameters into smaller, independent groups. LLM parameters are partitioned into contiguous blocks \mathcal{B}_i , each of a predefined size $d_1 \in \mathbb{N}^+$. Each block \mathcal{B}_i is then quantized independently using its own scale factor s_i and zero-point (denoted as z_i). Thus, for any parameter $w \in \mathcal{B}_i$, its quantized value q_w is given by $q_w = \mathcal{Q}(w; s_i, z_i)$, where $\mathcal{Q}(\cdot)$ is the quantization function. This allows for finer-grained adaptation to the local data distribution within each block.

The `q8_0`, `q5_0`, and `q4_0` methods employ symmetric quantization with a single-layer block structure, grouping 32 weights per block. These methods allocate 8, 5, and 4 bits to weight representation, respectively, while uniformly reserving 16 bits to store quantization parameters (scale and minimum values). Due to the additional bit overhead for shared scale parameters, the resulting BPW for `q8_0`, `q5_0`, and `q4_0` are calculated as 8.5, 5.5, and 4.5 bits, respectively.

Table 2: Selected quantization methods of llama.cpp

Series	Weight Component	Symmetric	d_1	d_2	Bits	s, m Bits	BPW
q8_0	All	✓	32	N/A	8	16	8.5
q5_0	All	✓	32	N/A	5	16	5.5
q4_0	All	✓	32	N/A	4	16	4.5
q5_k	attention.wv: Half	✓	16	16	6	8	6.5625
	feed_forward.w2: Half	✓	16	16	6	8	6.5625
	Others	✗	32	8	5	6	5.5
q4_k	attention.wv: Half	✓	16	16	6	8	6.5625
	feed_forward.w2: Half	✓	16	16	6	8	6.5625
	Others	✗	32	8	4	6	4.5
q3_k	attention.wv: All	✗	32	8	4	6	4.5
	attention.wo: All	✗	32	8	4	6	4.5
	feed_forward.w2: All	✗	32	8	4	6	4.5
	Others	✓	16	16	3	6	3.4375
q2_k	attention.wv: All	✗	32	8	4	6	4.5
	feed_forward.w2: All	✗	32	8	4	6	4.5
	Others	✗	16	16	2	4	2.5625

The remaining n_k quantization methods employ distinct precision-mixed strategies tailored to specific model components, featuring diverse block sizes and bit allocations for quantization parameters. As detailed in Table 2, the q5_k method utilizes symmetric quantization for half of the “attention.wv” and “feed_forward.w2” components, structured with a primary block (16 weights) and a secondary block (16 parameters). Here, weights and scale parameters are allocated 6 bits and 8 bits, respectively, resulting in a BPW of 6.5625. For asymmetric quantization, q5_k employs a 32×8 block configuration with 5 bits for weights and 6 bits for parameters, yielding a BPW of 5.5. The component-specific configurations in q4_k mirror those of q5_k, but with reduced bit allocations: 4 bits for weights and 6 bits for scale parameters, achieving a lower BPW of 4.5.

In the q3_k method, the components attention.wv, attention.wo, and feed_forward.w2 utilize a 32×8 block configuration, allocating 4 bits for weights and 6 bits for scale parameters, yielding 4.5 BPW. For other components, weights are quantized using a 16×16 block structure with 3 bits for weights and 6 bits for scale parameters, achieving a reduced BPW of 3.4375. The q2_k method adopts component-specific configurations analogous to q4_k and q5_k, but with distinct parameterizations. For attention.wv and feed_forward.w2, a 32×8 block is employed with 4 bits for weights and 6 bits for scale parameters. The remaining components leverage a 16×16 block structure, allocating 2 bits for weights and 4 bits for scale parameters, further optimizing the BPW metric.

A.3 Details of Metric Construction for Model Capability

For GSM8K [18], there are two types of matching scores: flexible-extract and strict-match. The former retrieves the last number in the response as the final answer to a mathematical question, disregarding the exact pattern of the answer. The latter one strictly matches the first number with a given pattern in the response. We use the maximum number between flexible-extract and strict-match matching scores as the evaluation metric.

For HumanEval [21], the model’s code completion ability is assessed using the pass@1 metric. It is given a function signature and a docstring describing the function, then tasked with completing it. The pass rate is determined by counting how many generated code snippets pass all test cases.

HellaSwag [19], MMLU [20], and TruthfulQA [22] are all multiple-choice evaluation tasks. Accuracy is determined by evaluating the model’s ability to select the correct answer from a set of predefined options. In HellaSwag [19] and MMLU [20], model capabilities are examined by presenting contextual information without explicit choices, utilizing the logits generated during inference to compute

Table 3: Performance of selected Llama 3 [17] instruction-tuned models.

Models & Tasks		Quantization							
		fp16	q8_0	q5_k	q5_0	q4_k	q4_0	q3_k	q2_k
3.1-8B	GSM8K [18]	/	77.94	77.33	76.57	76.42	76.80	71.95	46.17
	HellaSwag [19]	/	80.49	80.39	80.19	79.85	79.94	78.93	77.37
	MMLU [20]	/	68.42	68.25	68.22	67.57	66.99	66.47	59.46
	HumanEval [21]	/	62.80	63.41	62.20	61.59	61.59	61.59	43.29
	TruthfulQA [22]	/	54.40	54.09	54.42	53.53	52.13	52.78	45.68
3.2-3B	GSM8K [18]	64.90	65.28	65.28	66.26	63.91	61.64	59.89	24.41
	HellaSwag [19]	73.62	73.55	73.43	73.20	72.60	72.86	70.93	61.29
	MMLU [20]	60.83	60.75	60.44	60.30	60.08	59.72	57.09	46.52
	HumanEval [21]	50.61	48.78	50.61	49.39	51.22	50.61	47.56	26.83
	TruthfulQA [22]	51.46	51.66	51.82	50.91	52.09	50.26	66.34	45.85
3.2-1B	GSM8K [18]	35.03	35.25	34.80	32.75	32.07	30.78	26.91	2.96
	HellaSwag [19]	60.94	61.00	60.76	60.98	60.04	58.94	58.53	45.66
	MMLU [20]	46.27	46.35	45.91	45.94	44.29	44.40	43.11	31.35
	HumanEval [21]	34.15	34.15	35.98	32.93	31.10	29.27	26.83	4.88
	TruthfulQA [22]	43.39	43.52	43.43	43.47	44.24	43.51	40.86	42.48

the cumulative log probabilities for each candidate response. For TruthfulQA [22], we adopt the mc2 score to measure both truthfulness and informativeness, enabling the model to assign probability values to multiple correct answers.

A.4 Additional Results of Model Capability

We also showcase the performance of selected Llama 3 [17] instruction-tuned models, ranging in sizes from 1B to 8B parameters, across aforementioned tasks GSM8K [18], HellaSwag [19], MMLU [20], HumanEval [21], and TruthfulQA [22] in Table 3. Similar to the observations on Qwen 2.5 [16] models, we conclude that larger models in Llama 3 [17] demonstrate superior performance across all tasks compared to smaller models. For example, on GSM8K [18], the Llama 3.1 8B fp16 model achieves 78.01% accuracy, while the Llama 3.2 1B fp16 model reaches only 35.03%. Similar trends are observed across other benchmarks, reflecting the general advantage of model size in capturing and utilizing complex knowledge.

Within each model size, quantization levels significantly impact performance. Lower quantization levels (e.g. q3_k, q2_k) lead to noticeable performance declines. For instance, the Llama 3.1 8B model achieves 68.26% on MMLU [20] with fp16 but drops to 66.47% with q3_k and further plummets to 59.46% with q2_k. Similarly, for the Llama 3.2-1B model, accuracy on MMLU [20] decreases from 46.27% (fp16) to 43.11% (q3_k) and sharply to 31.35% (q2_k). The drop in quality at q2_k is particularly pronounced, emphasizing the limitations of extreme quantization.

Both Llama 3 [17] and Qwen 2.5 [16] consistently demonstrate that larger models outperform smaller ones across nearly all tasks. However, Qwen 2.5’s [16] 7B models surpass Llama 3 [17] 8B models on all five tasks, despite having a comparable number of parameters. Similar to Qwen 2.5 [16], Llama 3 [17] maintains stable performance with moderate quantization levels (e.g., q8_0, q5_k), but its accuracy degrades significantly under q2_k. Qwen 2.5 [16] models exhibit better resilience to quantization changes compared to Llama 3 [17]. For example, the Qwen 2.5 [16] 14B model on MMLU [20] shows only a minor drop from 79.74% (q5_k) to 78.86% (q3_k), whereas the Llama 3.1 8B [17] model experiences a sharper decline from 68.25% (q5_k) to 66.47% (q3_k). Furthermore, it is noticeable that the quantization q2_k of the Llama 3.2 1B model proves to be significantly ineffective for tasks such as GSM8K [18] and HumanEval [21].

A.5 Additional Results of Deployment Efficiency

The subsequent figures present further throughput results of LLMs with different quantization methods, employing selected quantization methods across input token lengths of 64, 256, and 512. The results consistently reveal a degradation in decoding throughput with increasing BPW, alongside

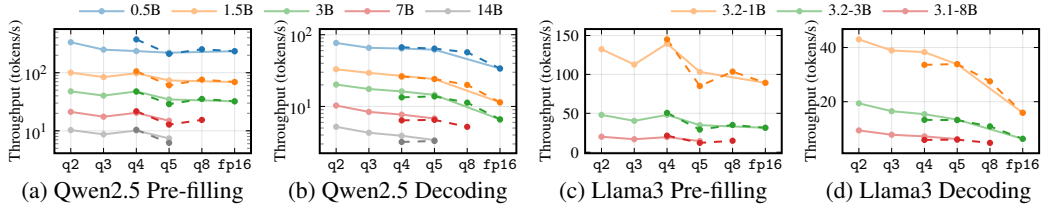


Figure 5: Pre-filling and decoding throughput of selected models of Qwen 2.5 [16] and Llama 3 [17] against different quantization methods (64-token input).

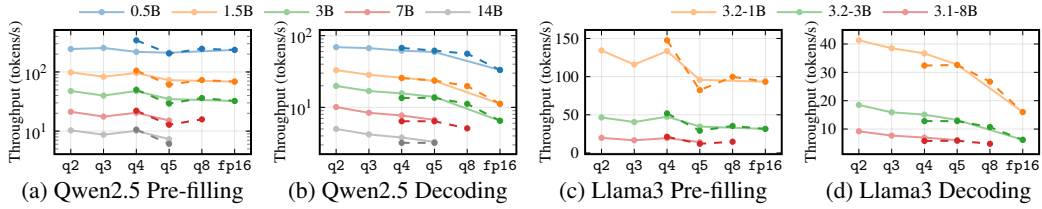


Figure 6: Pre-filling and decoding throughput of selected models of Qwen 2.5 [16] and Llama 3 [17] against different quantization methods (256-token input).

variations in pre-filling throughput linked to the operational complexity inherent in the quantization methods.

Further, the subsequent figures present additional results for LLMs across token lengths of 64, 256, and 512, employing quantization at 2-bit, 3-bit, 4-bit, and 8-bit precision levels. These results consistently reveal an exacerbated trend of throughput degradation with increasing model size, further underscoring the growing impact of computational bottlenecks at larger model scales. Notably, among 4-bit quantization methods, q4_0 exhibits superior throughput compared to q4_k, an advantage attributed to its implementation involving fewer CPU operations.

A.6 Additional Results of System Resource Utilization

To facilitate a detailed analysis of system resource utilization, additional metrics are collected using HWiNFO64. Following a warm-up phase utilizing q2_k quantization, inference scripts are sequentially executed on the Qwen 2.5 7B and Llama 3.1 8B models. These models are evaluated with a suite of quantization schemes: q2_k, q3_k, q4_k, q5_k, q4_0, q5_0, and q8_0. Each model instance underwent approximately 10 minutes of inference, employing 256 input tokens and generating 1000 output tokens.

Metrics, including CPU utilization, CPU frequency, and System Agent (SA) Power, are sampled using HWiNFO64. Key observations from this analysis are as follows: The pre-filling phase consistently exhibits significantly higher instantaneous power consumption compared to the decoding phase; however, average power consumption is predominantly dictated by the longer decoding phase. SA Power, an integral power management component within Intel CPU architectures responsible for regulating elements such as memory controllers, PCIe controllers, and display engines, effectively reflects memory access intensity and bandwidth utilization. Consequently, elevated SA Power levels observed with the q2_k, q3_k, and q5_0 quantization schemes are indicative of memory-bound workloads.

B Impact Statement

This paper presents work whose goal is to advance the field of deployment of LLM on resource constrained edge devices. There are many potential societal consequences of our work, none which we feel must be specifically highlighted here.

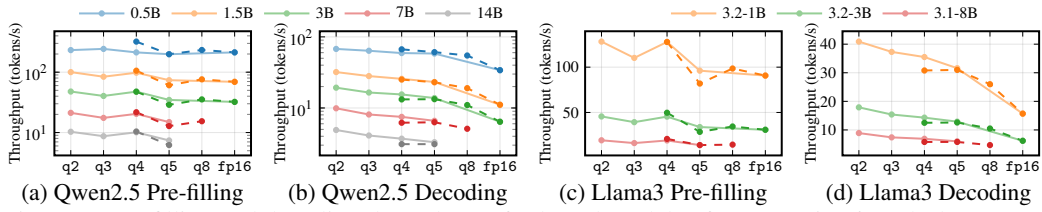


Figure 7: Pre-filling and decoding throughput of selected models of Qwen 2.5 [16] and Llama 3 [17] against different quantization methods (512-token input).

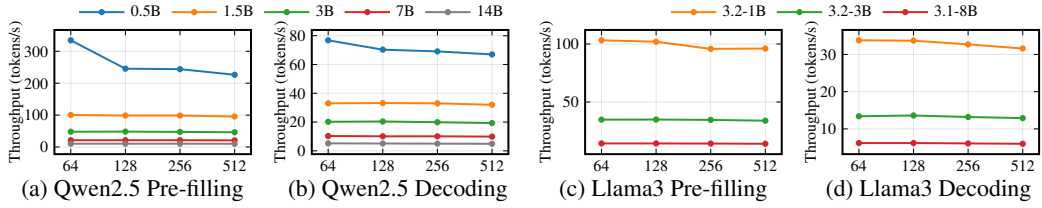


Figure 8: Pre-filling and decoding throughput with selected models of Qwen 2.5 [16] and Llama 3 [17] against different token lengths (q2_k quantization).

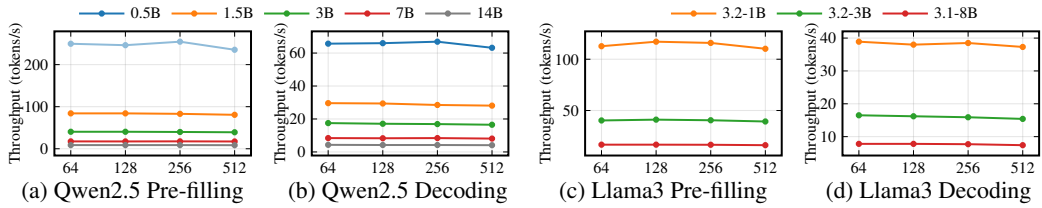


Figure 9: Pre-filling and decoding throughput with selected models of Qwen 2.5 [16] and Llama 3 [17] against different token lengths (q3_k quantization).

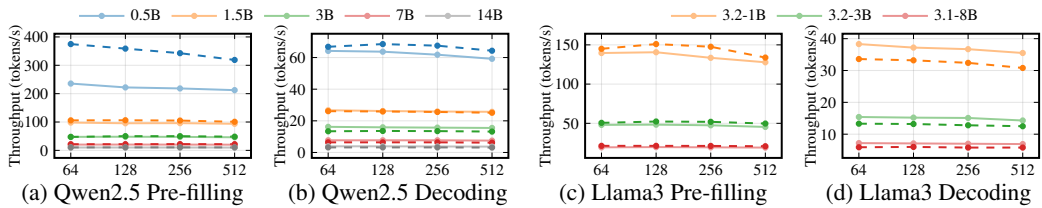


Figure 10: Pre-filling and decoding throughput with selected models of Qwen 2.5 [16] and Llama 3 [17] against different token lengths (4-bit quantization).

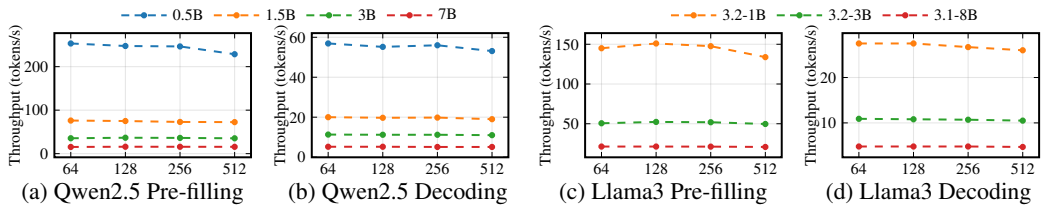


Figure 11: Pre-filling and decoding throughput with selected models of Qwen 2.5 [16] and Llama 3 [17] against different token lengths (q8_0 quantization).

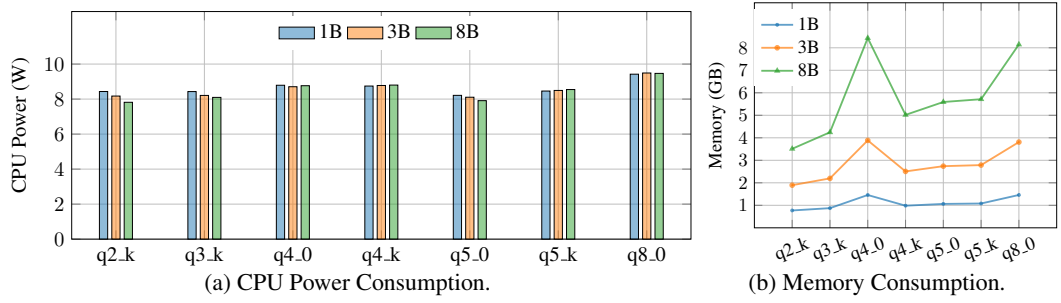


Figure 12: System resource utilization (power in Watt and memory in GB) of Llama 3 series (from 1B to 8B). Prompt size of 128 tokens and output size 1000 tokens are fixed.

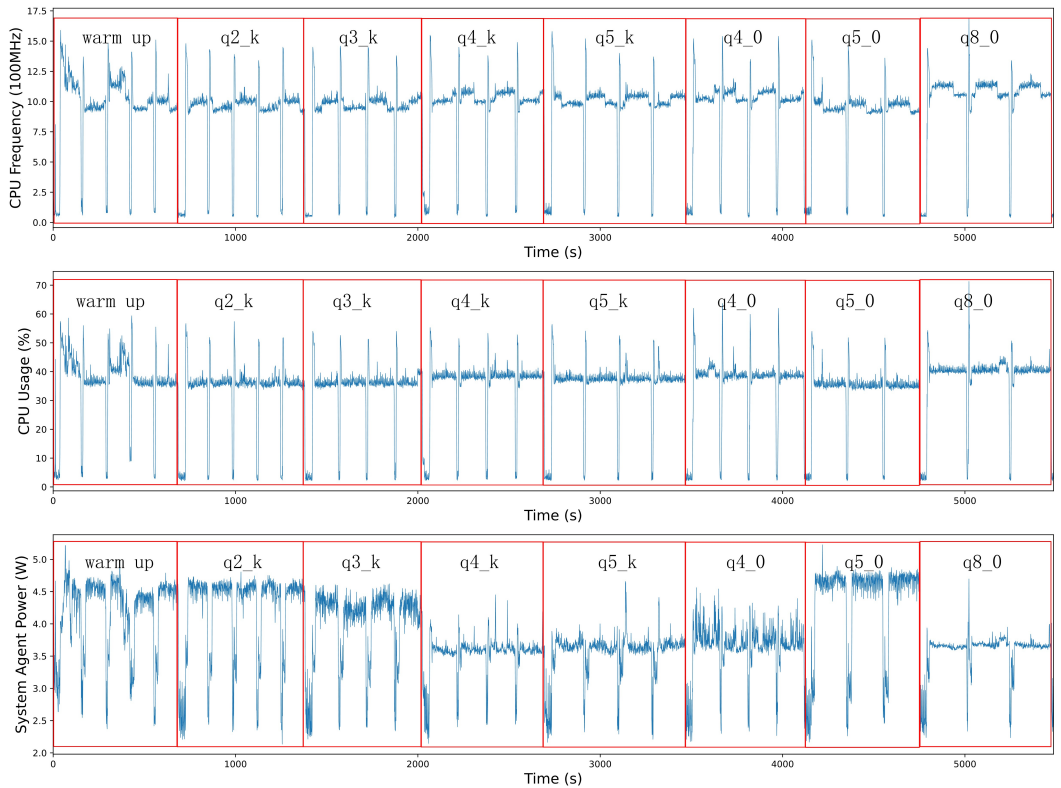


Figure 13: System resource utilization (CPU frequency in 100MHz, CPU utilization in percentage, system agent power in Watt) of Qwen 2.5 7B. Prompt size of 256 tokens and output size 1000 tokens are fixed.

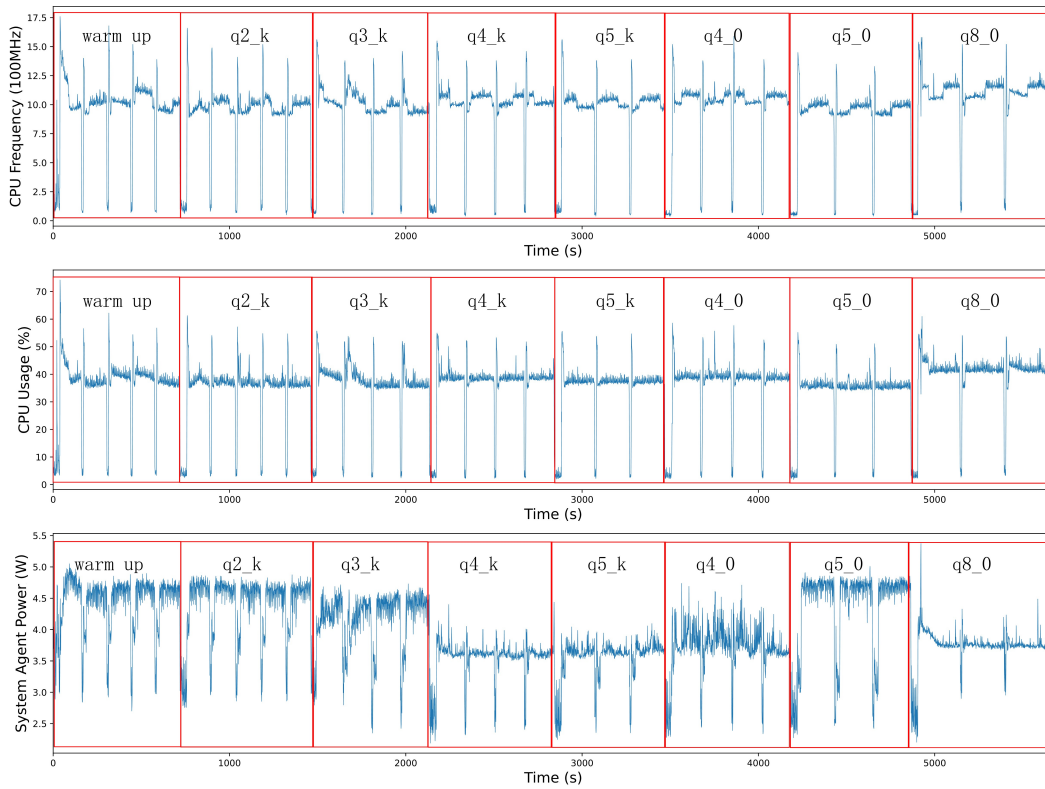


Figure 14: System resource utilization (CPU frequency in 100MHz, CPU utilization in percentage, system agent power in Watt) of Llama3.1 8B. Prompt size of 256 tokens and output size 1000 tokens are fixed.